J Intell Robot Syst (2014) 73:361–372
DOI 10.1007/s10846-013-9923-6

A Survey of Optical Flow Techniques for Robotics Navigation Applications

Haiyang Chao · Yu Gu · Marcello Napolitano

Received: 1 September 2013 / Accepted: 12 September 2013 / Published online: 12 October 2013

Abstract Optical flow has been widely used by insects and birds to support navigation functions. Such information has appealing capabilities for application to ground and aerial robots, especially for navigation and collision avoidance in urban or indoor areas. The purpose of this paper is to provide a survey of existing optical flow techniques for robotics navigation applications. Detailed comparisons are made among different optical-flow-aided navigation solutions with emphasis on the sensor hardware as well as optical flow motion models. A summary of current research status and future research directions are further discussed.

Keywords Optical flow · Robotics navigation · Unmanned aerial vehicles · Robotics sensing

H. Chao (✉)
Department of Aerospace Engineering,
University of Kansas, Lawrence, KS, 66045, USA
e-mail: chaohaiyang@ku.edu

Y. Gu · M. Napolitano
Department of Mechanical & Aerospace Engineering,
West Virginia University, Morgantown,
WV, 26505, USA

Y. Gu
e-mail: yu.gu@mail.wvu.edu

M. Napolitano
e-mail: marcello.napolitano@mail.wvu.edu

1 Introduction

Recent years have seen an exponentially increasing use of unmanned vehicles or robots for both military and civilian applications including but not limited to aerial surveillance, remote sensing, search and rescue, cargo delivery, bomb disposal, etc. However, most of the existing unmanned systems lack the intelligence to interact swiftly and efficiently with clustered, unstructured, and fast changing environments, such as many urban areas. Especially, several critical research challenges need to be addressed before the full integration of unmanned aircraft system (UAS) into the national airspace of the United States. Example challenges include sense and avoid capability, as well as navigation in GPS-degraded or GPS-denied environments. Currently, most small UAVs rely on GPS/Inertial Navigation System (INS) for navigation with no terrain or obstacle sensing ability [10]. However, such navigation solutions will not function properly for applications such as planetary exploration, indoor navigation, or under GPS spoofing scenarios. Moreover, the lack of "sense and avoid" collision avoidance capabilities poses great challenges for airspace sharing among manned and unmanned aircraft.

Optical flow techniques are natural solutions to the navigation and obstacle avoidance problem, as motivated by insect and bird flights. Optical flow can be treated as the projection of the 3D

perceived motion of objects, which has wide applications for motion estimation, video compression, and image interpolation. It has been discovered by biologists that honeybees rely on optical flows for grazing landing [9], travel distance estimation [14], obstacle avoidance, and flight speed regulation [49]. The compound eyes of insects such as dragonflies play an important role for these navigation functions with the capability of wide field motion detection [52].

Many different types of algorithms for optical flow computation have been developed by computer vision and biological experts, including gradient based approaches (e.g., Lucas-Kanade [36] and Horn-Shunck methods [25]), feature based methods (e.g., SIFT [35]), and interpolation techniques [48]. These algorithms can successfully generate optical flows with pixel level accuracy compared with the sub-pixel accuracy ground truth [3], using bench mark data sets collected by computer vision researchers.

Benefiting from prior work of biological and computer vision experts, robotics researchers have employed optical flow techniques to help solve the navigation and obstacle avoidance problem on ground and aerial robots. Various navigation subtasks have been accomplished with optical flow alone or coupled with inertial measurements, including ground odometry [26, 40], distance estimation [20], altitude hold and obstacle avoidance [5, 59], velocity and height estimation aided by inertial sensors [13, 47], and vertical landing [21], etc.

To support the above state estimation and autonomous navigation functions, both new vision systems and novel optical flow motion models have been developed. The two most commonly used sensors for generating optical flows are optical mouse chips and CCD/CMOS sensors. Several new vision systems have also been developed for specific features including omnidirectional vision system [46], specially designed vision chips for fast optical flow computation [8], binocular vision system [31], and wide-field optical flow approach [28].

Given optical flows computed from vision data, the associated optical flow motion field estimation models are required for navigation or sensor fusion purposes. Certain motion information such as rotational velocity, translational velocity, and terrain information can be estimated separately through the integration of optical flow with inertial, GPS, and range data. Two major groups of optical flow motion field estimation models have been proposed including pin-hole image surface approaches and spherical image surface approaches. The former approaches have the assumption of flat image surfaces, which is the case for most CCD sensors. Both narrow- and wide-field optical flows have been modeled [2, 11, 13, 37]. The latter approaches assume spherical image plane [28, 32], which is similar to the compound eyes of insect. This approach can be approximated by multiple low-resolution image chips at different viewing angles [57]. It is worth mentioning that most of the above researches assume static environments. Therefore, the optical flows are caused by the camera egomotion. Only several groups worked on the estimation of object motion using ground vehicles, which include the movements of the camera and the objects in the scene [19, 43].

This paper focuses on a survey of the optical flow related sensor hardware and the software, optical flow motion field estimation models, for robotics navigation purposes. A detailed comparison of different sensors and models is provided in terms of physical specifications as well as software strength and limitations.

The organization of this paper is described as follows. Section 2 provides the definition of optical flow and the inspirations for biorobotic approaches to the navigation problem. Section 3 gives a brief introduction on different algorithms for optical flow computation. Section 4 focuses on a detailed survey of existing optical-flow-aided navigation methods including both hardware and optical flow motion field estimation models. Section 5 describes the state of the art of optical-aided-navigation techniques for robotics applications and a prediction of the future research directions. Finally, conclusions are made in Section 6.

2 Optical Flow Definition & Biological Inspirations

There are two widely used definitions for optical flow including apparent motion definition and

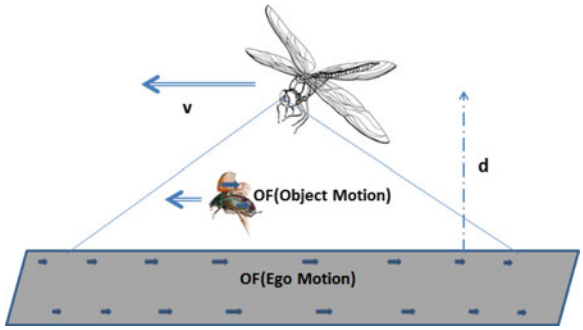

Fig. 1 The definition of optical flow

motion field definition [3]. Optical flow can be treated as the apparent motion of objects, brightness patterns, or feature points, observed from the eye or the camera. Following this definition, optical flow can be computed from the difference between two consequent images, which is usually expressed as

$$[\dot{\mu}, \dot{\nu}]^T = f(\mu, \nu)$$

for any point (μ, ν) on the image plane, with the unit of pix. per sec. or pix. per frame.

On the other hand, optical flow can also be defined as the projection of the relative 3D motion between the observer and the scene into the image plane. Such relative motion can usually be represented by associated motion field models, which will be described in detail in later sections. A simplified optical flow motion field model is described as the following and shown in Fig. 1:

$$\mathbf{OF}_m = \frac{\mathbf{v}}{d}, \tag{1}$$

where $\mathbf{OF}_m$ is the optical flow motion field, $\mathbf{v}$ is the observer velocity vector, d is the distance between the observer and the object along the optical axis. Following the motion field definition, optical flow is usually expressed in rad. per sec., or deg. per sec.. It is worth pointing out that the above two definitions are actually the same under ideal situations after coordinate transformation.

With the above definitions, associated motion information can be estimated from optical flow. In fact, optical flow incorporates information of both ego motion (EM) and object motion (OM). EM is defined as the movement of the observer with respect to the static environment, while OM means the movement of other independent objects. An example is the optical flow of a dragonfly, shown in Fig. 1. The optical flow field sensed by the dragonfly is actually a combination of ego-motion-induced flows from dragonfly movements and object-motion-induced flows from bug movements.

Optical flow has been discovered to be frequently used by birds and insects for short range navigation as well as obstacle avoidance through human controlled experiments by biologists and neural scientists [6, 17, 49]. It is observed that honeybees can achieve smooth landings and grazing behavior using optical flows, which require a variety of capabilities including ground speed keeping, wind disturbance rejection, collision avoidance, and auto takeoff/landing [49]. In recent years, researchers reported evidences that birds also use image motion or optical flow for obstacle avoidance and landing maneuver [6]. Additionally, optical flows are possibly used by many mam-

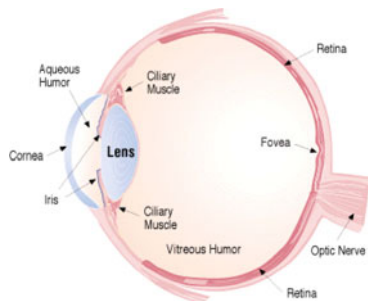

(a) Human eye. [51]

(b) Insect eye. [44]

Fig. 2 Single chambered eyes and compound eyes

mals for the motion detection of object motion as well [43, 55].

The new discoveries on optical flow from biological society provide new ideas to robotics researchers toward developing robots with agile visuo-motor capability for the safe and fast navigation of unstructured and clustered environments. Researchers have built new bioinspired systems including both sensor hardware and fusion algorithms to mimic biological vision systems in the nature. The two major directions are to simulate single chambered eyes and to simulate compound eyes, shown in Fig. 2. Birds, human beings all have single chambered eyes, which can provide high-accuracy images. Robotics applications using high-resolution cameras all fall in this category. However, advanced sensor fusion algorithms are needed for the computation of optical flow. Another direction is to simulate the compound eyes of insects, starting from the simulation of a single neuron sensor. A survey along both directions are provided in the later sections in detail.

3 Optical Flow Computation from Computer Vision

Optical flow can be calculated from the movement of objects with the same brightness value or feature pattern between two consequent images. The optical flow field across the whole image plane can be further expressed as a function of image pixels, $f(\mu, \nu)$, or a function of azimuth and elevation angles, $g(\psi, \theta)$.

There are many algorithms to determine optical flow from video sequences, benefiting from early works of image processing and computer vision communities. Most of the optical flow computation algorithms have the following assumptions [7, 41]:

- Brightness/feature constancy: only the movement of the object with respect to the camera can cause local changes of the image intensity/feature;
- Spatial smoothness: the motion is uniform over a small neighborhood of pixels;
- Small motion: the sampling frequency of the video is fast enough to represent the image motion gradually over time.

These assumptions can be written in the following equation, assuming that $I(\mu, \nu, t)$ is the light intensity function, or the feature function of a point (μ, ν) on the 2D image plane at time t:

$$I(\mu, \nu, t) = I(\mu + \delta\mu, \nu + \delta\nu, t + \delta t), \tag{2}$$

$$I_\mu \dot{\mu} + I_\nu \dot{\nu} + I_t = 0. \tag{3}$$

With the above assumptions, many algorithms have been developed by computer vision researchers for the computation of optical flows, including differential methods [36, 53], region-based matching methods [1], energy-based methods, phase-based methods [16], fusion-based methods [50], fractional-order-operator-based method [12], etc. A comprehensive survey and comparison of different optical flow algorithms can be found in [3, 4].

Several representative optical flow algorithms used by robotics communities are introduced in the following:

- Lucas-Kanade method, which is one of the differential methods for optical flow computation with local energy optimization [36]. The differential methods compute optical flow from spatiotemporal derivatives of image intensity or filtered image [4]. Lucas-Kanade algorithm is robust to image noise, but may not generate dense flows [4];
- Horn-Schunck method, which is also a differential method but with global energy minimization [25]. This method is more sensitive to noise, but can generate dense flow fields [4];
- Image interpolation method, which is developed by Srinivasan specially for low-computation applications such as small UAVs [48]. This method does not need tracking of features or calculation of image velocity at different locations [58];
- Block matching algorithm, which include methods to minimize the sum of squared differences (SSD) or the sum of absolute difference (SAD). SAD block matching method has been incorporated with inertial

measurements for accurate estimation of optical flow on small UAVs [30];
- Feature-based methods, features can be used instead of the raw intensity values for the computation of optical flow. Feature extraction algorithms such as Scale Invariant Feature Transform (SIFT) can be used to detect features. The detected features are then further correlated into pixel movements representing optical flow [35].

In recent years, several bench mark data sets have been collected and shared by computer vision researchers for optical flow algorithm validation purposes [3]. These data sets include nonrigid motions as well as substantial motion discontinuities. Many optical flow algorithms have been observed to be able to achieve sub-pixel level accuracy compared with the ground truth data [3]. However, these videos only include much slower motions, which is not common for typical UAV flights.

4 Optical Flow for Navigation

With the emerging of efficient optical flow algorithms and miniature sensor hardware, researchers begin to use optical flow to support navigation of ground robots as well as fixed-wing and rotary-wing UAVs in the last two decades. A comprehensive investigation of exiting researches on optical-flow-based robotics navigation is provided in this section with an emphasis on both the sensor hardware and associated reference motion models.

4.1 Optical Flow Sensor Hardware

Many different types of vision sensor hardware have been used for the collection of videos to generate optical flow. The sensor needs to be small in size and light due to the constraints of small or micro robotics platforms. More importantly, the hardware limitations of different vision sensors can greatly affect the consequent optical flow computation. For instance, the pixel count has a direct impact on the computational power required for onboard optical flow computation while the field of view (FOV) affects the sensing range of the robot. A detailed comparison of characteristics of optical flow sensor hardware is introduced in detail in the following.

Optical mouse sensors are the most widely used sensors for optical flow measurements in robotics applications. They can support an image sampling rate as fast as 1000 frames per second or higher [20, 31]. Optical mouse sensors are especially sensitive to changes in height above surfaces, which can in turn be used to estimate the distance to the object [20]. Similarly, CentEye Inc. has developed a series of vision chips to support embedded vision applications with asynchronous interface, shutterless pixel circuits, and flexible pixel window downsampling [8]. The CentEye 16×32 pix chip has been reported to be able to acquire the image and calculate the optical flow at a speed as fast as 545 frame per second [34]. CentEye chips have been used on small UAVs for obstacle avoidance and hovering flight [8].

In addition to the above COTS vision sensors, researchers have also developed nontraditional vision systems, inspired by bird or insect eyes:

- Omnidirectional vision system: a novel mirror profile was designed by researchers from University of Queensland for the acquisition of omnidirectional images to support the UAV navigation [46].
- Binocular vision system: research groups at Australian National University have integrated the optical flows measured from a pair of optical chips at different heights for the estimation of height, velocity and attitude [31].
- Wide-field optical flow: wide-field optical flow has been proposed to mimic compound eyes of insects such as dragonflies, honeybees, or fruit flies, for complex terrain following [45, 57].

In recent years, several research groups have combined vision systems with traditional navigation sensors to form coupled optical flow and inertial navigation system. A comparative study has shown the feasibility of integrating optical flow with traditional navigation sensors from flight test data of a fixed-wing

Table 1 Specification comparison of different vision sensors

Sensor type	Image pixel	Size	Weight	Update rate	FOV	Applications
ADNS-2610 [20]	18 × 18 pix.	25 × 30 mm	15 g	1500 Hz	6.5 deg.	Obstacle avoidance
(with lens)		35 × 30 mm	23 g	20 Hz (OF)	2.5 deg.	
		50 × 30 mm	23 g		1.2 deg.	
CentEye TinyTam	16 × 16 pix.	7 × 7 mm	125 mg	20Hz (OF)	N/A	VTOL UAV Hovering
Stonyman	112 × 112 pix.	2.8 × 2.8 mm	N/A	N/A	N/A	
Hawksbill	136 × 136 pix.	2.3 × 32.7 mm	N/A	N/A	N/A	
OV7740+FPGA [56]	320 × 240 pix.	6.5 × 6.5 × 4 mm (camera only)		120 Hz	50 deg.	Onboard OF calculation
PX4FLOW [24]	188 × 120 pix.	45.5 × 35 mm		250/500 Hz	21 deg.	Onboard OF calculation
	120 × 32 pix.	45.5 × 35 mm		250/500 Hz	180 deg.	
GoPro Hero [11]	1920 × 1080 pix.	42 × 60 × 30 mm	94 g	29.97 Hz	127 deg.	Compare w. navigation
	1280 × 720 pix.	42 × 60 × 30 mm	94 g	59.94 Hz	170 deg.	sensors

UAV platform [11]. Another example is the PX4FLOW Smart Camera developed for Quad-Rotor navigation applications by ETH, which provides onboard optical flow estimates after corrections for rotations [24]. Similar solutions include customer designed GPU-FPGA system for real-time onboard estimation of optical flows [23, 56].

The detailed specifications of several representing vision sensors are listed in Table 1. In the update rate column, two types of rates are listed including the image acquisition rate (IM) and the optical flow computation rate (OF). It can be observed that most of the former work on optical-flow navigation used relatively low or medium resolution vision sensors (300 × 200 pix. or less) due to the real-time considerations.

4.2 Optical Flow Motion Field Estimation Models

Optical flow motion field estimation models are defined as the projection of the 3D relative motion into the 2D image plane. In theory, the motion field should match the apparent motion of brightness/feature pattern. The obtained motion field estimates can serve as a reference for optical flows computed from vision, which is similar to the ground truth in computer vision societies [3].

The navigation information contained in optical flow include rotational velocities (p, q, r), translational velocities (u, v, w) and terrain information, all expressed in the camera body frame. The information flow from traditional navigation sensors to optical flow estimates is shown in detail in Fig. 3. The derived optical flows $(\dot{\mu}, \dot{\nu})$ is expressed as $f(\mu, \nu)$, a function of the pixels across the image plane.

There are generally two major approaches for deriving the motion field estimation models, pin-hole image plane approach and spherical imaging surface approach, which are inspired by biological vertebrate eyes and compound eyes respectively.

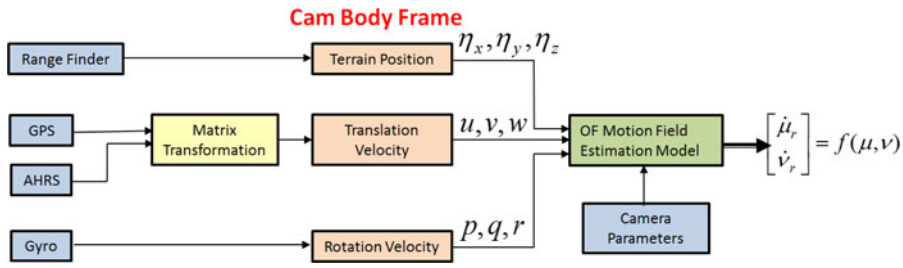

Fig. 3 Optical flow motion model for integration of navigation information

4.2.1 Pin-Hole Image Plane Approach

Pin-hole image plane approaches include motion models acquired through the assumption of the pin-hole camera model, which fits most COTS vision sensors. The pin hole camera model is used to map a point (η_x, η_y, η_z) in the 3D camera body frame $(\mathcal{F}_c)$ into the 2D image plane $(\mathcal{P}_i)$ with coordinates (μ, ν). $\mathcal{F}_c$ is centered at the camera aperture with the optical axis as z axis, $\mathcal{P}_i$ is centered at the intersection of the optical axis and the image plane. The mapping is shown in Fig. 4 with the image plane on the same side of the object instead of the opposite side for simplicity reasons. The mapping function from $\mathcal{F}_c$ to $\mathcal{P}_i$ using pin hole model can be described as follows:

$$\mu = f\frac{\eta_x}{\eta_z}, \tag{4}$$

$$\nu = f\frac{\eta_y}{\eta_z}, \tag{5}$$

where f is the focal length. Note that the focal length f and μ/ν need to be expressed in the same unit, which could be either in pixels or in millimeters.

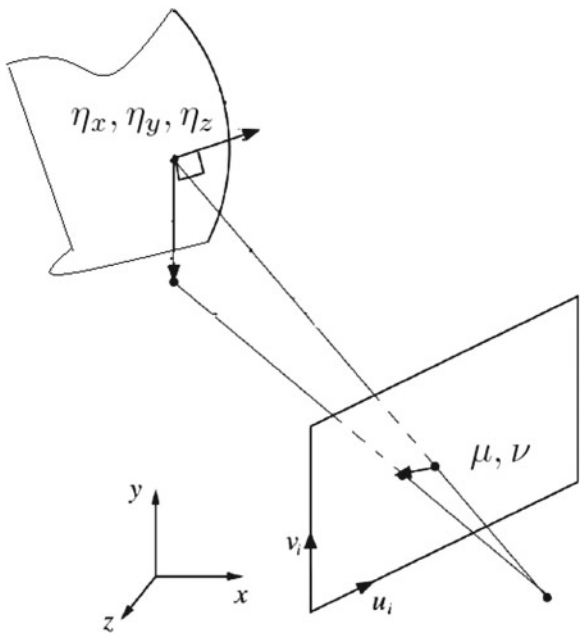

Fig. 4 Optical flow projection to flat imaging surface

The optical flow estimates can be acquired through the derivative of μ, ν.

$$\begin{bmatrix}\dot{\mu}\\ \dot{\nu}\end{bmatrix} = f\begin{bmatrix}\frac{1}{\eta_z} & 0 & -\frac{\eta_x}{\eta_z^2}\\ 0 & \frac{1}{\eta_z} & -\frac{\eta_y}{\eta_z^2}\end{bmatrix}\begin{bmatrix}\dot{\eta}_x\\ \dot{\eta}_y\\ \dot{\eta}_z\end{bmatrix}, \tag{6}$$

The following equations have been proposed to calculate the optical flows $\dot{\mu}$ and $\dot{\nu}$, based on previous works at WVU [37, 38], which is also similar to the results from other researchers [2, 29]:

$$\begin{bmatrix}\dot{\mu}\\ \dot{\nu}\end{bmatrix} = f\begin{bmatrix}\frac{1}{\eta_z} & 0 & -\frac{\eta_x}{\eta_z^2}\\ 0 & \frac{1}{\eta_z} & -\frac{\eta_y}{\eta_z^2}\end{bmatrix}[{}^C V_{B/C} + {}^C\omega_{B/C} \otimes ({}^C P - {}^C O_B)], \tag{7}$$

where ${}^C V_{B/C}^T$ is the translational ground velocity expressed in the camera frame $\mathcal{F}_c$, ${}^C\omega_{B/C}$ is the angular velocity with respect to the camera frame $\mathcal{F}_c$, ${}^C O_B$ is the rotation center, ${}^C P$ is the feature point expressed in $\mathcal{F}_c$.

The optical flow equations for the downward looking camera is further derived in the following, considering the available sensor suites for UAVs [11]. The vision sensor is assumed to be mounted at the center of gravity of the UAV such that the x and y axes of the 2D image plane coincides with the x and y axes of the vehicle body frame.

$$\begin{bmatrix}\dot{\mu}\\ \dot{\nu}\end{bmatrix} = \begin{bmatrix}f\frac{u}{\eta_z} - \frac{\mu w}{\eta_z}\\ f\frac{v}{\eta_z} - \frac{\nu w}{\eta_z}\end{bmatrix} + \begin{bmatrix}fq - r\nu - \frac{p}{f}\mu\nu + \frac{q}{f}\mu^2\\ -fp + r\mu - \frac{p}{f}\nu^2 + \frac{q}{f}\mu\nu\end{bmatrix}, \tag{8}$$

where p, q, r are angular rates measured by gyroscopes, u, v, w are ground velocity expressed in the camera body frame, η_z is the z direction distance in camera body frame F_C, μ, ν are pixel distance to the image center in the 2D image plane, and $\dot{\mu}, \dot{\nu}$ are optical flows usually expressed in pixels per frame or pixels per second.

Considering only the area close to the center ($\mu \approx 0, \nu \approx 0$), the optical flow motion model can be simplified as:

$$\begin{bmatrix} \dot{\mu}_c \\ \dot{v}_c \end{bmatrix} = \begin{bmatrix} f\dfrac{u}{\eta_z} \\ f\dfrac{\dot{v}}{\eta_z} \end{bmatrix} + \begin{bmatrix} fq \\ -fp \end{bmatrix}. \tag{9}$$

Similar equations have been used by other researchers for integration of optical flow and GPS/INS for UAV navigation [13].

For ground robots, Eq. 10 can be simplified to

$$\begin{bmatrix} \dot{\mu} \\ \dot{v} \end{bmatrix} = f \begin{bmatrix} \dfrac{1}{\eta_z} & 0 \\ 0 & \dfrac{1}{\eta_z} \end{bmatrix} \begin{bmatrix} \dot{\eta}_x \\ \dot{\eta}_y \end{bmatrix},$$

assuming a flat surface. Therefore, optical flow can be integrated together with accelerometer measurements for the velocity and odometry estimation. Extended Kalman filters are usually designed to compensate for vision noises and multiple optical flow readings [26, 40, 47].

4.2.2 Spherical Imaging Surface Approach

Instead of assuming a flat imaging surface, optical flows can also be modeled using spherical imaging surface, similar to a biological compound eye. Here, the conversion is needed from a flat image plane to a spherical retina [54].

Assume the image surface of the camera is spherical with unit image radius. For any target pint P (η_x, η_y, η_z) in the camera frame, the corresponding image point p in the spherical surface can then be expressed as [21]:

$$p = \frac{P}{\|P\|}. \tag{10}$$

The optical flow, or the image derivative $\dot{p}$ can be calculated by [21, 32]:

$$\dot{p} = -\Omega \times p - \frac{\pi_p}{\|P\|}(V - V_P), \tag{11}$$

where π_p is the projection from the 3D camera body frame to the tangent space of the spherical surface, V is the vehicle translational velocity, V_P is the target translational velocity. The optical flow projection to the spherical imaging surface is shown in Fig. 5, which is taken from [21].

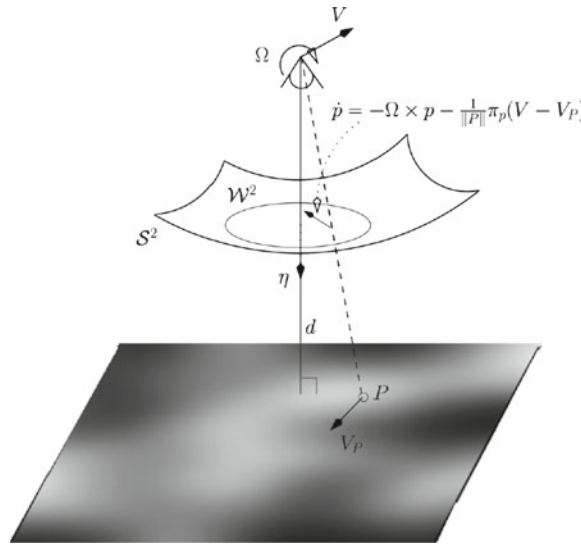

Fig. 5 Optical flow projection to spherical imaging surface [21]

Similar derivations have been employed by other researchers for the model of wide field optical flows. Given a spherical frame centered at the vantage point, the optical flow can be modeled using the following equation for the downward looking camera [28]:

$$\mathbf{OF} = -\boldsymbol{\omega} \times \mathbf{r} - \kappa[\mathbf{v} - (\mathbf{v} \cdot \mathbf{r})\mathbf{r}], \tag{12}$$

$$\kappa(\gamma, \beta, \mathbf{q}) = \frac{s\beta(s\phi c\theta s\gamma - s\theta c\gamma) + c\beta c\phi c\theta}{h_D - z}, \tag{13}$$

$$\mathbf{q} = [x, y, z, \phi, \theta, \psi]. \tag{14}$$

where $\mathbf{r} = (\gamma, \beta)$ is a unit vector representing the direction from image surface to the vantage point, γ, β are the azimuth and elevation angles, κ is a nearest function (downward looking for aircraft), $\mathbf{v}$ and $\boldsymbol{\omega}$ are velocity and angular velocity measurements respectively.

Spherical image surface model has been used many researchers due to its simplicity to be used on 1D camera or optical flow sensors [59]. The disadvantage is that the azimuth and elevation angle representation has to be converted into a flat surface for direct 2D video applications.

4.2.3 Other Motion Field Estimation Models

Other than the above approaches considering wide field of view (FOV), optical flows can also be estimated from optical mouse sensors or other similar sensors with narrow FOV. Agilent ADNS-2610 optical mouse sensors have been installed on MAVs to estimate the distance to the obstacles in flights [20]. Such sensors only has small field of view ($< 6.5°$ FOV) and small footprint (18×18 pixels) [20]. The outputs of such sensors are δp_x and δp_y, representing the optical flow across the sensor's field of view in longitudinal and lateral directions. The distance to the obstacle in the field of view can be described as below [20]:

$$D = d\cos(\phi)\sin(\alpha),$$
$$d = \frac{V_{gps}T_s}{\tan\frac{\lambda_{eff}}{2}},$$
$$\lambda_{\text{eff}} = \lambda_{\text{cam}}\frac{\delta p_x}{P_x} - \dot{\chi}\,T_s, \tag{15}$$

where λ_{eff} is the effective field of view, λ_{cam} is the field of view of the camera, $\dot{\chi}$ is the yaw rate with respect to the ground, P_x is the size of the pixel array, T_s is the flight time. Other researchers have used similar methods on video streams [31].

5 Current Status and Future Research Directions

In summary, many researchers from biological, computer vision, robotics, and aerospace societies have contributed to this area along different directions such as understanding bird or insect flights, invention of new vision systems, development of optical flow estimation algorithms, and improvement of optical flow motion field estimation models, etc. Optical flow and related vision systems have been frequently used on ground and aerial robots for different navigation tasks including:

1. Distance estimation: researchers from Brigham Young University achieved canyon following using a small flying-wing UAV platform, aided from the obstacle sensing capability provided by a series of optical mouse sensors mounted at different viewing angles [20].
2. Altitude hold and obstacle avoidance: optical flow has also been used as the direct feedback to micro UAVs for altitude maintain and yaw control to avoid obstacles by researchers from EPFL and University of Maryland [5, 59].
3. Velocity and height estimation aided by inertial sensors: optical flow measurements combined with inertial readings can provide robust estimation of ground velocity and flight height during GPS dropouts [13].
4. 2D ground velocity estimation and vision odometry: optical flow measurements from single or multiple vision sensors can be combined with inertial measurements to provide estimation of ground velocity as well as 2D positions [26, 40, 47].
5. Hovering and terrain following: optical flow has been used to provide an estimation of horizontal velocity with respect to the ground. The obtained velocities and integrated positions can then be used for hovering control [18, 27, 39, 42].

Table 2 Comparison of different optical-flow-based navigation approaches

Navigation functions	Authors	Robotic platform	OF computation	Model
Landing on moving platform	ONERA-UNICE-ANU [21]	Quad-Rotor	Lucas-Kanade	(11)
Velocity/Height estimation	UNSW-ADFA-UTS [13]	Helicopter	Image interpolation algo.	(9)
Obstacle avoidance	BYU [20]	Flying-Wing	Outputs from mouse sensor	(15)
Obstacle avoidance altitude keeping	EPFL [58, 59]	Ultra light MAV	Image interpolation algo.	(11)
Horizontal velocity estimation hovering	UAEH-UTC [39]	Eight-Rotor VTOL	Lucas-Kanade	(9)
Vision odometry velocity estimation	ETHZ [24]	Quad-Rotor	SAD block matching	(8)
OF comparison: vision vs navigation sensors	WVU [11]	Small Fixed-Wing	Sift feature	(8)

6. Vertical landing: optical flow measurements can also be directly used as a feedback for the landing task of VTOL UAVs, mimicking the grazing landing of honeybees. Researchers have shown the feasibility of optical-flow-based stabilization and landing on a moving platform [21, 22], which has many maritime and military applications.

A summary of the above works is provided in detail in Table 2. It can be observed that several different types of algorithms are used for optical flow computation in the robotics community. Among them is the Lucas-Kanade algorithm which has the most applications due to its simple implementation and low computational requirements. Another observation is that most of the recent optical flow navigation algorithms were tested using VTOL UAVs for indoor applications, with few researches on fixed-wing UAV platforms or ground vehicles.

In summary, all the above approaches have shown great potentials of optical flows to be widely employed to increase the sensing and navigation capabilities of UAVs or micro ground robots. However, many challenges need to be addressed for the real industrial application of optical-flow-aided navigation system.

1. Quantitative evaluation of optical flow systems: there are very few works focusing on the quantitative evaluation of optical flow for robotics navigation and obstacle avoidance purposes. Researchers from computer vision societies have proposed several benchmark data sets together with evaluation methodologies for comparison of different algorithms. Similar ideas can be adapted to the robotics navigation problem with the introduction of new metrics for performance and robustness of optical flow systems. Besides, both indoor and outdoor evaluations under different terrain and light conditions need to be focused.
2. Real-time optical flow from high-resolution images: most current robots are already equipped with high-resolution cameras for surveillance tasks. The large amount of video data has potentials to be used for optical flow computation with the help from new processing units such as GPUs. It is worth mentioning here computer vision scientists have developed real-time SIFT computation algorithms using powerful GPUs [33] or with faster parallel methods [15].
3. Novel vision systems for more accurate and robust optical flows: most birds and insects have two eyes or compound eye to sense the external world. Similarly, multiple vision sensors can be installed on UAVs and new algorithms are needed for the wise integration of multiple vision sources with inertial or range measurements.

6 Conclusions

This paper provides a comprehensive survey of vision sensor hardware and reference motion models for using optical flows to support robotics navigation. Several representing examples for optical-flow-based navigation of both ground and aerial unmanned vehicles were looked into including obstacle avoidance, terrain following, vertical landing, velocity estimation, visual odometry, etc. Although many researchers have achieved one or several of the above navigation functions, most of the results are still either limited to structured indoor environments or constrained by computation powers. In addition, quantitative evaluation and systematic calibration of existing optical-flow-based navigation systems are needed before real-world applications.

Acknowledgements This work was partially supported by NASA grant # NNX10AI14G. The authors want to thank the anonymous reviewers for providing valuable comments to help improve the quality of this paper.

References

1. Anandan, P.: A computational framework and an algorithm for the measurement of visual motion. Int. J. Comput. Vis. **2**(3), 283–310 (1989)
2. Arvai, A., Kehoe, J., Lind, R.: Vision-based navigation using multi-rate feedback from optic flow and scene reconstruction. Aeronaut. J. **115**(1169), 411–420 (2011)
3. Baker, S., Scharstein, D., Lewis, J., Roth, S., Black, M.J., Szeliski, R.: A database and evaluation methodology for optical flow. Int. J. Comput. Vis **92**(1), 1–31 (2011)

4. Barron, J., Fleet, D., Beauchemin, S.: Performance of optical flow techniques. Int. J. Comput. Vis **12**(1), 43–77 (1994)
5. Barrows, G., Neely, C., Miller, K.: Fixed and flapping wing aerodynamics for micro air vehicle application, vol. 23, chap. Optic Flow Sensors for MAV Navigation, pp. 557–573. AIAA (2001)
6. Bhagavatula, P.S., Claudianos, C., Ibbotson, M.R., Srinivasan, M.V.: Optic flow cues guide flight in birds. Curr. Biol. **21**, 1794–1799 (2011)
7. Black, M.J., Anandan, P.: The robust estimation of multiple motions: parametric and piecewise-smooth flow fields. Comp. Vis. Image Underst. **63**(1), 75–104 (1996)
8. CentEye Inc.: Cent eye website. http://embeddedeye.com/profiles/blogs/open-source-xmos-daughter (2012)
9. Chahl, J., Srinivasan, M.V., Zhang, S.W.: Landing strategies in honeybees and applications to uninhabited airborne vehicles. Int. J. Robot. Res. **23**(2), 101–110 (2004)
10. Chao, H., Cao, Y., Chen, Y.Q.: Autopilots for small unmanned aerial vehicles: a survey. Int. J. Control Autom. Syst. **8**(1), 36–44 (2010)
11. Chao, H., Gu, Y., Gross, J., Guo, G., Fravolini, M.L., Napolitano, M.R.: A comparative study of optical flow and traditional sensors in UAV navigation. In: Proceedings of the 2013 American Control Conference. Washington DC (2013)
12. Chen, D., Sheng, H., Chen, Y., Xue, D.: Fractional-order variational optical flow model for motion estimation. Phil. Trans. R. Soc. A 107–117 (2013). doi:10.1098/rsta.2012.0148
13. Ding, W., Wang, J., Han, S., Almagbile, A., Garratt, M.A., Lambert, A., Wang, J.J.: Adding optical flow into the gps/ins integration for UAV navigation. In: Proceedings of the International Global Navigation Satellite Systems Society IGNSS Symposium. Holiday Inn Surfers Paradise, Qld, Australia (2009)
14. Esch, H.E., Burns, J.E.: Distance estimation by foraging honeybees. J. Exp. Biol. **199**, 155–162 (1996)
15. Feng, H., Li, E.Q., Chen, Y., Zhang, Y.: Parallelization and characterization of sift on multi-core systems. In: IEEE International Symposium on Workload Characterization, pp. 14–23 (2008)
16. Fleet, D., Jepson, A.: Computation of component image velocity from local phase information. Int. J. Comput. Vis. **5**(1), 77–104 (1990)
17. Franceschini, N.: Visual Guidance Based on Optic Flow: A biorobotic approach. J. Physiol. Paris **98**(13), 281–292 (2004)
18. Garratt, M.A., Chahl, J.S.: Vision-based terrain following for an unmanned rotorcraft. J. Field Robot. **25**(7), 284–301 (2008)
19. Giachetti, A., Campani, M., Torre, V.: The use of optical flow for road navigation. IEEE Trans. Syst. Man Cybern. Part B Cybern. **14**(1), 34–48 (1998)
20. Griffiths, S., Saunders, J., Curtis, A., Barber, B., McLain, T., Beard, R.: Maximizing miniature aerial vehicles: obstacle and terrain avoidance for mavs. IEEE Robot. Automat. Mag. **13**(3), 34–43 (2006)
21. Herisse, B., Hamel, T., Mahony, R., Russotto, F.X.: Landing a VTOL unmanned aerial vehicle on a moving platform using optical flow. IEEE Trans. Robot. **28**(1), 77–89 (2012)
22. Herisse, B., Russotto, F.X., Hamel, T., Mahony, R.: Hovering flight and vertical landing control of a VTOL unmanned aerial vehicle using optical flow. In: Proceedings of the IEEE International Conference on Intelligent Robotics and Systems, pp. 801–806. Nice, France (2008)
23. Honegger, D., Meier, L., Tanskanen, P., Greisen, P., Pollefeys, M.: Real-time velocity estimation based on optical flow and disparity matching. In: Proceedings of the IEEE International Conference on Robotics and Automation. Vilamoura, Algarve, Portugal (2012)
24. Honegger, D., Meier, L., Tanskanen, P., Pollefeys, M.: An open source and open hardware embedded metric optical flow cmos camera for indoor and outdoor applications. In: Proceedings of the IEEE International Conference on Robotics and Automation. Karlsruhe, Germany (2013)
25. Horn, B., Schunck, B.: Determining optical flow. Artif. Intell. **17**, 185–203 (1981)
26. Hu, J.S., Chang, Y.J., Hsu, Y.L.: Calibration and on-line data selection of multiple optical flow sensors for odometry applications. Sensors Actuators A Phys. **149**(1), 74–80 (2009)
27. Humbert, J.S., Murray, R.M., Dickinson, M.H.: Pitch-altitude control and terrain following based on bio-inspired visuomotor convergence. In: Proceedings of the AIAA Guidance, Navigation, and Control Conference. San Francisco, CA, USA (2005)
28. Hyslop, A.M., Humbert, J.S.: Autonomous navigation in three-dimensional urban environments using wide-field integration of optic flow. J. Guid. Control Dyn. **33**(1), 147–159 (2011)
29. Kehoe, J.J., Watkins, A.S., Causey, R.S., Lind, R.: State estimation using optical flow from parallax-weighted feature tracking. In: Proceedings of the AIAA Guidance, Navigation, and Control Conference. Keystone, Colorado, USA (2006)
30. Kendoul, F., Fantoni, I., Nonami, K.: Optic flow-based vision system for autonomous 3d localization and control of small aerial vehicles. Robot. Auton. Syst. **57**(6), 591–602 (2009)
31. Kim, J., Brambley, G.: Dual optic-flow integrated navigation for small-scale flying robots. In: Proceedings of the Australasian Conference on Robotics and Automation. Brisbane, Australia (2007)
32. Koenderink, J.J., van Doorn, A.J.: Facts on optical flow. Biol. Cybern. **56**(4), 247–254 (1987)
33. Lalonde, M., Byrns, D., Gagnon, L., Laurendeau, D.: Real-time eye blink detection with gpu-based sift tracking. In: Fourth Canadian Conference on Computer and Robot Vision (2007)
34. Leonard, A.: Embedded eye blog. http://centeye.com/ (2012)
35. Lowe, D.G.: Distinctive image features from scale-invariant keypoints. Int. J. Comput. Vis. **60**(2), 91–110 (2004)

36. Lucas, B.D., Kanade, T.: An iterative image registration technique with an application to stereo vision. In: Proceedings of the 1981 DARPA Image Understanding Workshop (1981)
37. Mammarella, M., Campa, G., Fravolini, M., Gu, Y., Seanor, B., Napolitano, M.: A comparison of optical flow algorithms for real time aircraft guidance and navigation. In: Proceedings of the AIAA Guidance, Navigation, and Control Conference. Honolulu, HI, USA (2008)
38. Mammarella, M., Campa, G., Fravolini, M., Napolitano, M.: Comparing optical flow algorithms using 6-dof motion of real-world rigid objects. IEEE Trans. Syst. Man Cybern. Part C Appl. Rev. **42**(6), 1752–1762 (2012)
39. Romero, H., Salazar, S., Lozano, R.: Real-time stabilization of an eight-rotor UAV using optical flow. IEEE Trans. Robot. **25**(4), 809–817 (2009)
40. Ross, R., Devlin, J., Wang, S.: Toward refocused optical mouse sensors for outdoor optical flow odometry. IEEE Sensors J. **12**(6), 1925–1932 (2012)
41. Roth, S., Black, M.J.: On the spatial statistics of optical flow. Int. J. Comput. Vis **74**(1), 33–50 (2007)
42. Ruffier, F., Franceschini, N.: Optic flow regulation: the key to aircraft automatic guidance. Robot. Auton. Syst. **50**(7), 177–194 (2005)
43. Schmüdderich, J., Willert, V., Eggert, J., Rebhan, S., Goerick, C., Sagerer, G., Körner, E.: Estimating object proper motion using optical flow, kinematics, and depth information. IEEE Trans. Syst. Man Cybern. B Cybern. **38**(4), 1139–1151 (2008)
44. Shahan, T.: Compound eyes of a robber fly. http://www.flickr.com/photos/opoterser/3085177911/ (2013)
45. Slatyer, E., Mahony, R., Corke, P.: Terrain following using wide field optic flow. In: Proceedings of the Australasian Conference on Robotics and Automation. Brisbane, Australia (2007)
46. Soccol, D., Thurrowgood, S., Srinivasan, Y.: A vision system for optic-flow-based guidance of UAVs. In: Proceedings of the Australasian Conference on Robotics and Automation. Brisbane, Australia (2007)
47. Song, X., Seneviratne, L.D., Althoefer, K.: A kalman filter-integrated optical flow method for velocity sensing of mobile robots. IEEE/ASME Trans. Mechatronics **16**(3), 551–563 (2011)
48. Srinivasan, M.V.: An image interpolation technique for the computation of optical flow and egomotion. Biol. Cybern. **71**, 401–415 (1994)
49. Srinivasan, M.V.: Honeybees as a model for the study of visually guided flight, navigation, and biologically inspired robotics. Physiol. Rev. **91**, 389–411 (2011)
50. Sun, J., Shum, H.Y., Zheng, N.: Stereo matching using belief propagation. IEEE Trans. Pattern Anal. Mach. Intell. **25**(7), 787–800 (2003)
51. The human eye. https://www.sabic-ip.com (2013)
52. Torii, A., Imiya, A., Sugaya, H., Mochizuki, Y.: Optical flow computation for compound eyes: Variational analysis of omni-directional views. Brain Vis. Artif. Intell. Lect. Notes Comput. Sci. **3704**, 527–536 (2005)
53. Tretiak, O., Pastor, L.: Velocity estimation from image sequences with second order differential operators. In: Proceedings of the International Conference on Pattern Recognition. Montreal, Canada (1984)
54. Vassallo, R.F., Santos-Victor, J., Schneebeli, H.J.: A general approach for egomotion estimation with omnidirectional images. In: Proceedings of the Third Workshop on Omnidirectional Vision. Washinton DC, USA (2002)
55. Warren, P.A., Rushton, S.K.: Optic flow processing for the assessment of object movement during ego movement. Curr. Biol. **19**, 1555–1560 (2009)
56. Watman, D., Murayama, H.: Design of a miniature, multi-directional optical flow sensor for micro aerial vehicles. In: Proceedings of the IEEE International Conference on Robotics and Automation. Shanghai, China (2011)
57. Zufferey, J.C., Beyeler, A., Floreano, D.: Autonomous flight at low altitude using light sensors and little computational power. Int. J. Micro Air Veh. **2**(2), 107–117 (2010)
58. Zufferey, J.C., Floreano, D.: Optic-flow-based steering and altitude control for ultra-light indoor aircraft. Report LIS-REPORT-2004-001, EPFL (2004)
59. Zufferey, J.C., Floreano, D.: Toward 30-gram autonomous indoor aircraft: vision-based obstacle avoidance and altitude control. In: Proceedings of the IEEE International Conference on Robotics and Automation, pp. 2594–2599. Barcelona, Spain (2005)